ARTICLE IN PRESS

ELSEVIER

Journal of Arid Environments ▮ (▮▮▮▮) ▮▮▮–▮▮▮

Journal of Arid Environments

www.elsevier.com/locate/jnlabr/yjare

Ground temperature measurement and emissivity determination to understand the thermal anomaly and its significance on the development of an arid environmental ecosystem in the sand dunes across the Israel–Egypt border

Z. Qin[a,c,*], P.R. Berliner[b], A. Karnieli[b]

[a] *International Institute for Earth System Science, Nanjing University, Nanjing 210093, China*
[b] *J. Blaustein Institute for Desert Research, Ben Gurion University of the Negev, Sede Boker Campus 84990, Israel*
[c] *MOA Key Laboratory of Resource Remote Sensing and Digital Agriculture, Chinese Academy of Agricultural Sciences, Beijing 100081, China*

Received 23 May 2003; received in revised form 15 March 2004; accepted 29 March 2004

Abstract

The Israel–Egypt border region composed of longitudinal sand dunes is a very unique arid environmental ecosystem in the world: the Israeli side with much more vegetation cover has notably higher land surface temperature (LST) during daytime than the Egyptian side where bare sand prevails. In order to understand this thermal anomaly and its scientific significance in the arid environmental ecosystem development, a series of intensive research activities have been conducted in the past several years, including remote sensing analysis and meteorological modeling. In the paper, we present part of the series studies on the issue: the ground temperature measurement and emissivity determination. The region is mainly composed of four basic surface patterns: biogenic crust, bare sand, vegetation and playa (physical crust). Our hypothesis to occurrence of the thermal anomaly is that it is the direct result of the different surface composition structures and ground emissivities on both sides. Results from our ground temperature measurements during 1997–1998 validate the hypothesis of a significant LST difference existing among the main surface patterns of the region. Biogenic crust covering 72% on the Israeli side and only about 12% on the Egyptian side has an

*Corresponding author. International Institute for Earth System Science, Nanjing University, Nanjing 210093, China.
E-mail address: qinzh@nju.edu.cn (Z. Qin).

0140-1963/$ - see front matter
doi:10.1016/j.jaridenv.2004.03.017

average kinetic surface temperature of above 3°C higher than bare sand. Emissivity of the two most important surface patterns also presents a significant difference. Biogenic crust has an average emissivity ranging from 0.9671 at low temperature to 0.9725 at high temperature. Bare sand occupying above 80% of the surface on the Egyptian side and only about 7% on the Israeli side has an average emissivity between 0.9435 and 0.9543. On the basis of the ground temperature measurements, we use the estimated surface cover percentage to factor the emissivity for a simple simulation of average LST on both sides, which results in an outcome that strongly support the explanation of the thermal anomaly in the border region. Since biogenic crust that covers most surface of the region plays important functions in arid ecosystem development and is common in several deserts such as north Africa and central Australia, our documentation of its surface temperature change and determination of its emissivity, which have not been seen in the literature, will provide valuable scientific basis for other studies on arid environmental ecosystems.

Keywords: Land surface temperature; Israel–Egypt border; Emissivity; Biogenic crust; Sand; Remote sensing

1. Introduction

A unique landscape ecosystem was found in the arid region across the Israel–Egypt political border. Geomorphorlogically, the region is composed of the longitudinal sand dunes stretching from the Egyptian Sinai into the Israeli Negev. The formation of the sand dunes in the region were mainly due to the deposition of fine sand and dust transported from North African desert by strong wind. The unique characteristics of the arid ecosystem lie not only in its sharp spectral contrast between the two sides of the border (Fig. 1a) but also the obvious land surface temperature anomaly across the border (Fig. 1b). On remote sensing images (such as Fig. 1a) of visible channels, this region is characterized by a sharp contrast between bright reflectance from the Egyptian side (Sinai) and dark one from the Israeli side (Negev) (Pinker and Karnieli, 1995; Tsoar and Karnieli, 1996; Qin et al., 2001). The bright reflectance of the Egyptian side is a result of its more bare ground due to the intensive land use by Bedouin nomads. In contrast, the Israeli side is under conservation of restrictive land use policy, which allows the free development of high vegetation and biogenic crust having low spectral reflectance. As a result of relatively more vegetation cover, the Israeli side should be cooler than the Egyptian side. This has been the case across the border between USA and Mexico (Balling, 1989; Balling et al., 1998). However, an opposite thermal change is observed on the daytime thermal images of the Israel–Egypt border region. The Israeli side has notably higher land surface temperature (Qin et al., 2001, 2002a). This phenomenon can be observed almost throughout the year except for several days after heavy rain when the ground is very wet and cool. Considered denser vegetation cover on the Israeli side that could have stronger evapo-transpiration to cool down surface temperature, this phenomenon of temperature difference across the border can be termed as

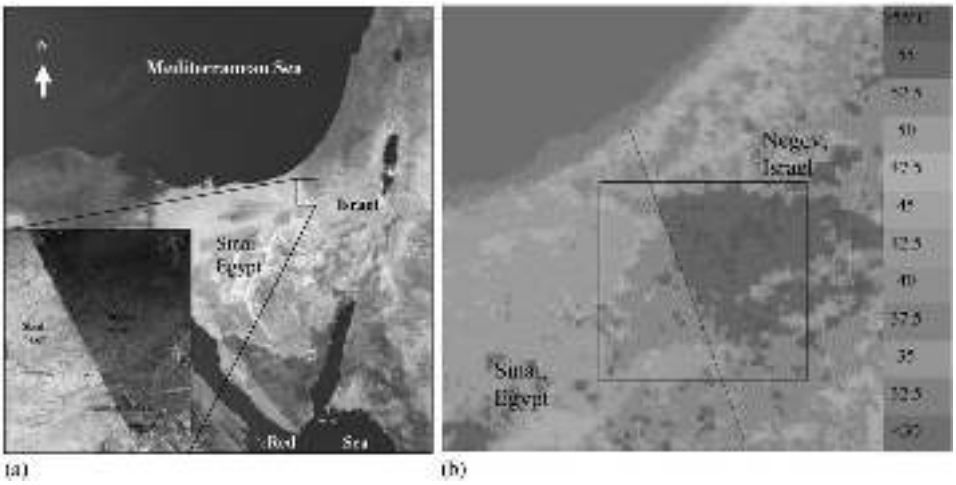

Fig. 1. Visible band image showing the geographical location of the study (a) and the land surface temperature variation of the region (b). Both are NOAA-AVHRR images. The insert in (a) is a Landsat TM image. Land surface temperature in image (b) is computed from the channels 4 and 5 of the AVHRR data acquired on July 18, 1998 at 12:08 GMT or 3:08 pm local time using split window algorithm given in Qin et al. (2002a).

anomalous. In order to provide a scientific explanation to this interesting thermal phenomenon and to examine its significance in arid ecosystem development, a series of intensive investigation activities have been done from both remote sensing analysis and micrometeorological modeling. The current paper intends to present the ground emissivity determination and ground temperature measurement of the main surface patterns in the region, which is an undividable part of the investigation. Ground emissivity and temperature are two important thermal parameters of ecosystem. They are required for both remote sensing analysis and micrometeorological modeling to understand the functioning of the arid ecosystem in this particular region.

In contrast to the very few examinations of the thermal anomaly, the sharp spectral difference across the visible border has been extensively and intensively studied for understanding its natural process of occurrence and its ecological implication. The spectral difference of the arid ecosystem on both sides of the border region was first reported and interpreted by Otterman (1974). Since then, a number of scientific efforts have been devoted into further examination of the phenomenon from various viewpoints (Otterman, 1977, 1981; Otterman and Robinove, 1982; Otterman and Tucker, 1985; Warren and Harrison, 1984; Tsoar and Møller, 1986, pp. 75–95; Danin, 1991; Karnieli and Tsoar, 1995; Pinker and Karnieli, 1995; Tsoar and Karnieli, 1996; Karnieli, 1997; Tielböger, 1997). In his early article, Otterman (1974) observed the contrast in the first Landsat MSS image of the region taken in 1972 and pointed out that semi-dormant desert fringe plants strongly reduced the albedo of sandy terrain. He stated that green plants would have produced a Sinai–Negev contrast ratio much higher in the MSS visible bands and particularly the red

band (600–700 nm), where plant chlorophyll strongly absorbs solar radiation. The contrast was therefore interpreted as a product of dark plant debris and shadowing effects. Karnieli and Tsoar (1995) suggested a different interpretation to the spectral contrast. After examining the difference of vegetation cover and biogenic crust cover and the spectral reflectance of the arid dune vegetation and biogenic crust, they concluded that the well-known contrast between Sinai and Negev in remote sensing imagery that had drawn the attention of many scientists was not a direct result of vegetation cover difference but caused by almost a complete cover of biogenic crust in the Israeli Negev and the scarcity of the crust in the Egyptian Sinai (Karnieli and Tsoar, 1995). The change of the spectral reflectance values on remote sensing between 1984 and 1989 was depicted in another article of the two authors (Tsoar and Karnieli, 1996) using Landsat MSS data. They attributed to the decrease of the brightness value in all Landsat MSS bands except the NIR (near infrared band 7) to probable effect of further destruction of vegetation in Sinai after 1982. Using the remote sensing data of both NOAA-AVHRR and Landsat TM, Qin et al. (2002a) gave a detailed examination of the thermal anomaly phenomenon from remote sensing analysis. Surface kinetic temperature difference across the border has been estimated from NOAA-AVHRR and Landsat TM data. The estimated temperature difference can be 2.5–3.5°C during dry summer (Qin et al., 2002a). The mechanism leading to the thermal contrast on both sides has been simulated using a micrometorological model based on surface energy balance in Qin et al. (2002b). Influences of such factors as soil water content, albedo, radiation, wind speed, air temperature, relative humidity, and so on have been analysed in the simulation. The result from the simulation indicates that the albedo difference between biogenic crust and bare sand is the main factor contributing to their surface temperature difference. Land cover percentage of the main surface patterns has been quantitatively estimated in Qin et al. (2003) with three methods: field observation, measurement on aerial photograph and validation on Landsat TM image. According to the simulation and considering the obvious quantity difference of the two surface on both sides, Qin et al. (2002a) suggested that the observed LST on remote sensing images was mainly due to the difference of land cover structure, especially the difference of biogenic crust and bare sand on both sides.

The sand dune region across the political border is mainly composed of four surface patterns: biogenic crust, bare sand, vegetation and playa. Field observation indicates that the Israeli side is mainly covered with biogenic crust and vegetation, while the Egyptian side is dominant with bare sand. Biogenic crust with thickness of 1–5 mm is a common surface pattern in many arid environments such as Sahara and central Australia. It plays important functions in arid ecosystem development. The crust is a direct result of the activities of cyanobacteria and other microphytes in active sand dunes. While growing, cyanobacteria produce a kind of sticky silk that holds sand together. Thus, development of the crust is the first step for sand dune ecosystem changing from active sand into fixed sand so that other plants can settle on (Danin, 1991; Karnieli and Tsoar, 1995; Karnieli et al., 1996; Karnieli and Sarafis, 1996). Fine sand with low quartz content and light yellow color (Tsoar, 1990; Gerson et al., 1985) is the main soil constituent in the region though silt and clay also

accounts some percentages ($<5\%$) especially on the Israeli side where a thin biogenic crust cover about 72% of its surface (Qin et al., 2003). In this paper, we intend to report the result of our experimental determination of ground emissivity in the region as well as ground temperature measurements of the main surface patterns. Since biogenic crust that covers most surface of the region plays important functions in arid ecosystem development and is common in several deserts of the world, our documentation of its surface temperature change and determination of its emissivity, which have not been seen in the literature, will provide valuable scientific basis for other studies on arid ecosystems. Using a thermal radiance model, we also perform an estimation of the average surface temperature on both sides of the border according to the available data of ground emissivity and land cover structure. The estimation is oriented to the ground temperature measurements for verifying the satellite-observed thermal anomaly across the border.

2. Determination of ground emissivity

Emissivity is an important factor that affects the observed surface temperature change through detecting the thermal radiance of the object under study. The ground surface is not a black body. Most natural objects are able to emit only part of its potential radiant energy (Caselles et al., 1997). Therefore, the direct output of temperature measurement by an infrared (IR) thermometer (or a remote sensing system) can only give the radiant (apparent) temperature change of the objects. In order to know the true or kinetic temperature change of the ground, surface emissivity is necessary for correcting the observed radiant temperature. Moreover, the retrieval of LST from remote sensing data (mainly NOAA-AVHRR and Landsat TM in our study) in the series investigation also requires the known of surface emissivity. These requirements make the determination of ground emissivity necessary in the study.

2.1. Method and experiments

Though several methods have been proposed (Humes et al., 1994; Labed and Stoll, 1991a), directly measuring emissivity of the ground surface in the field is still very difficult due to the cost and the instrumental system. The general way for emissivity determination in an acceptable economic level is to take the soil samples from the field and carry out experiments for the determination. And we also follow this in the study. The soil samples for the experiments were taken from the field during the wet season of 1997/98 using metal cans. We took the sampling for several times: on January 16 and 26, and March 19 and 26, 1998. Great cares were exerted when taking the samples in order to avoid soil structure change. The samples were air-dried on the shelf of our laboratory to compare the surface condition in dry season of the region.

Biogenic crust and bare sand are the most important surface compositions of the region and together they account for above 85% of the area. The emissivity of

biogenic crust on the surface of sandy soil has not been yet reported. Though several studies such as Sobrino and Caselles (1991) and Sabins (1996) stated that sand (mainly quartz) has an emissivity of 0.91–0.92, the emissivity of fine sand in the region, which is mainly composed of dust and rocky particles (Gerson et al., 1985), have also not been studied. Therefore, we focus our experiments on determining the emissivity of these two surface patterns. The emissivity of vegetation has been reported (Humes et al., 1994; Labed and Stoll, 1991a) and that of playa, due to its composition, can be viewed as having similar soil properties with silt and clay.

The principle of determining emissivity through laboratory experiments is to compare the difference of radiant temperature between the measured samples and their reference black body. The experiments were conducted with the use of a water bath with constant temperature inside and an IR thermometer operating in 8–14 μm to measure the radiant temperature of the samples. A circulator was installed in the water bath to keep the temperature constant. On the top of the bath is a moveable semi-transparent cover so that the samples in the bath can be seen. The cover also acts as an isolated layer to prevent the impact of thermal radiance from environment on the samples. There is a small hole on the cover to mount the sensor of the thermometer for measuring the radiant temperature of the samples under study.

The soil samples were arranged to float on the water surface of the bath. Five typical sand samples and five typical biogenic crust samples were selected for the measurement. At the same time, a reference with black surface was also put in the bath. Then a semi-transparent cover was used to cover the bath to isolate the bath from environment. The IR thermometer was mounted on the small hole of the cover. A datalogger with storage was connected to the thermometer for data recording. After the samples were put in the bath for more than 2 h, we started to measure the temperatures of the samples and the reference through operating the cover with the thermometer over them. The output of the thermometer was recorded by a datalogger. Data output frequency of thermometer was set into one reading per second. The thermometer has the ability to react with the thermal radiance in 2–3 s. For each sample, we took the measurement for 10–20 s so that we would have about 15 temperature readings of the sample. The samples were measured one by one and we repeated the measurements for five times. Three temperature treatments (25°C, 35°C and 45°C) were used for the experiments in order to represent three circumstances of surface temperature change in the region. In summer, surface temperature of the region is usually high up to above 45°C and in winter it is about 25°C for most days.

The emissivity of the samples can be determined on the basis of the assumption that the samples and the black body reference have the same kinetic temperature. Because the thermometer was mounted just on top of the bath with a distance of less than 15 cm from the samples and a cover was used to isolate the bath from its environment, the possible effects of environmental emittance from air and the laboratory walls in detecting their surface temperature can be minimized and hence ignored. In order to get an average measurement the temperatures of the samples and the black reference were measured in an iterative way for five times.

Consequently, the observed difference of the radiant temperatures among the samples can be assumed to be the direct result of their emissivity difference.

The IR thermometer measures the radiant temperature of the samples by detecting their thermal radiance. Actually the thermal radiance reaching the IR sensor is not only the emittance from the sample, but also the effects from the environment. Because the samples are not black bodies with emissivity of 1, they have ability to reflect the downward thermal radiance from the air and the indoor laboratory wall. And the air between the sensor and the sample surface also has ability to emit some thermal radiance to reach the IR sensor. Thus we have total thermal radiance reaching the IR sensor as

$$I = I_s + I_r + I_a^{\uparrow}, \tag{1}$$

where I is the total thermal radiance reaching the sensor; I_s is the thermal emittance from the sample; I_r is the reflected downward thermal radiance from air, and laboratory walls and ceiling; and $I_a^{\uparrow}$ is the upward air emittance. Since we used a cover to isolate the bath from environment, we successfully minimized the effects of thermal radiance from laboratory walls and ceiling on the measurements. Now we only need to consider the downward and upward air emittances. Because our sensor is only about 15 cm from the sample surface, the air transmittance τ_λ within the thin layer can be termed as $\tau_\lambda \approx 1$. Accordingly, both upward and downward air emittances can be computed as

$$I_r = (1-\varepsilon)I_a^{\downarrow} = (1-\varepsilon)(1-\tau_\lambda)B_\lambda(T_a^{\downarrow}) \approx 0, \tag{2}$$

$$I_a^{\uparrow} = (1-\tau_\lambda)B_\lambda(T_a^{\uparrow}) \approx 0, \tag{3}$$

where $B_\lambda(T_a)$ is the Planck radiance function with wavelength λ and temperature T_a. Thus, we have $I \approx I_s$ in our case.

Total emittance of a black body with temperature T_b can be estimated as Stefan–Boltzmann function or Planck function. With Stefan–Boltzmann function, the emittance can be computed as

$$I(T_b) = \sigma T_b^4, \tag{4}$$

where $I(T_b)$ is the emittance of the body at temperature T_b, σ is the Stefan–Boltzmann constant with $\sigma = 5.67 \times 10^{-8}\,\mathrm{W\,m^{-2}\,K^{-4}}$. With Planck function, we have

$$I(T_b) = \frac{1}{\lambda_2 - \lambda_1}\int_{\lambda_1}^{\lambda_2} \frac{c_1}{\lambda^5(e^{c_2/(\lambda T_b)} - 1)} f(\lambda)\,d\lambda, \tag{5}$$

where c_1 and c_2 are the first and the second radiance constants with $c_1 = hc^2 = 5.95522012 \times 10^{-17}\,\mathrm{W\,m^2}$ and $c_2 = hc/k = 1.43876869 \times 10^{-2}\,\mathrm{m\,K}$, λ is the wavelength, and $f(\lambda)$ is the spectral response function of the instrument within its wavelength range between λ_1 and λ_2. Since Stefan–Boltzmann function is about the entire wavelength and our instrument is only for the wavelength of 8–14 μm, we prefer to select Planck function for the determination of emissivity. The soil sample with temperature T_0 is not a black body and only has an emittance of $I(T_0) = \varepsilon I(T_b)$.

Thus, its emissivity can be computed as

$$\varepsilon = \frac{I(T_0)}{I(T_b)} = \frac{\int_{\lambda_1}^{\lambda_2} \frac{c_1}{\lambda^5(e^{c_2/(\lambda T_0)} - 1)} f(\lambda)\,d\lambda}{\int_{\lambda_1}^{\lambda_2} \frac{c_1}{\lambda^5(e^{c_2/(\lambda T_b)} - 1)} f(\lambda)\,d\lambda}, \quad (6)$$

where T_b and T_0 are the measured temperature (K) of black body and the sample.

Black body is only a theoretical concept and there is no absolute black body in nature. Thus, we assume that the black body reference has an emissivity of 0.999. Using this assumption, the temperature of the black body reference is firstly calibrated into its real kinetic temperature. Another consideration in the determination is the possible error resulted from both instruments and operation. Because the bath is set for constant temperature, the true temperature of the black body reference should be the same as the constant temperature in the bath. Usually there is a slight difference from the expected constant temperature. Therefore, calibration has to be done before the above formula is used to calculate the emissivity. In practice, the difference between the temperature of the black body reference and the expected constant temperature is used as the calibration coefficient.

2.2. Results and analysis

The results of emissivity determination are shown in Fig. 2 and the detailed calculation is given in Table 1 for the treatments of 25°C and 45°C. Fig. 2 indicates that biogenic crust has higher emissivity than sand. According to the experiments, the average emissivity of the five samples at 25°C is 0.9660 for the biogenic crust and 0.9388 for the bare sand. The difference is about 0.0272. T-test yields $T_{stat} = 8.00 > T_{\alpha=0.01} = 3.36$, indicating the difference is statistically significant at the level $\alpha = 0.01$. The average emissivity at 35°C is 0.9695 for the biogenic crust and 0.9460 for the sand, with a difference of 0.0235, which is statistically significant ($T_{stat} = 6.15$). At 45°C treatment, the average emissivity of biogenic crust and sand is 0.9729 and 0.9552 separately, with a difference of 0.0178, which is also statistically significant ($T_{stat} = 3.87$). For the sand dune region, LST is usually between 35°C and 50°C at about noon. Therefore, it can be concluded that the surface emissivity is about 0.97 for the biogenic crust and about 0.95 for the bare sand, with a difference of about 0.02 in the region.

Soils may have great difference of emissivity due to the difference in their properties. Many studies reported that bare silt soil has an emissivity of 0.96–0.98 and sandy soil 0.93–0.96 (Hausenbuiller, 1978; Brutsaert, 1982; Labed and Stoll, 1991a, b; Humes et al., 1994). Biogenic crust in the region is actually composed of silt, fine sand, microphytes, fungus and some debris of plants such as the death roots of annuals. The grain size of the sand in the region is also very fine (about 0.1–0.5 mm). The color of the sand is light yellow. The mineral components of sand are mainly the dust and rocky particles from the North African desert. Quartz percentage of the sand is less than 50% in weight (Gerson et al., 1985). According to

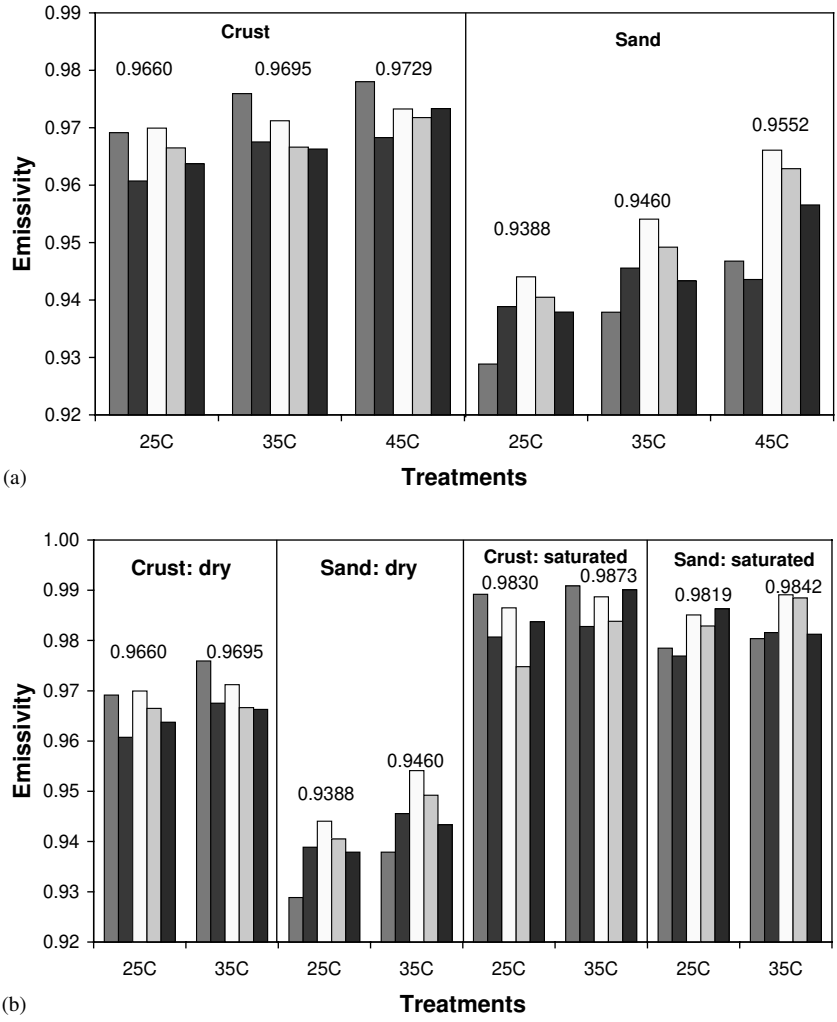

Fig. 2. Emissivity of the biogenic crust and the sand samples, illustrating (a) its variation for various temperature treatments and (b) its comparison in dry and saturated conditions. The number in the graph is the average emissivity of the samples for the treatment.

the soil properties of the region and compared with the reported soil emissivity in the literature, it can be said that the results of our experiments are acceptable.

Two more features can also be seen from this change of soil emissivity in the experiments. Firstly, emissivity of the samples increases gradually with temperature. For biogenic crust, the emissivity increases from 0.9660 at 25°C to 0.9729 at 45°C. For sand it changes from 0.9388 to 0.9552. The weak increase feature of soil emissivity with temperature has been mentioned in many studies (Hillel, 1980; Brutsaert, 1982; Sobrino et al., 2001) and our experimental results correspond very

Table 1
Computation of emissivity based on laboratory experimental data

Samples	Treatment at 25°C			Treatment at 45°C		
	Temperature (K)		Emissivity	Temperature (K)		Emissivity
	Measured	Calibrated		Measured	Calibrated	
Reference	297.9306	298.1600	1.00	318.4227	318.1600	1.00
Crust 1	295.6622	295.8854	0.96915	316.5995	316.3368	0.97800
Crust 2	295.1044	295.3276	0.96075	315.8766	315.6139	0.96829
Crust 3	295.7156	295.9388	0.96995	316.1875	315.9848	0.97326
Crust 4	295.4868	295.7100	0.96650	316.1371	315.8744	0.97178
Crust 5	295.3035	295.5267	0.96374	316.2540	315.9913	0.97335
Average	295.4545	295.6777	0.96602	316.2110	315.9482	0.97294
Sand 1	292.9589	293.1821	0.92885	314.2584	313.9957	0.94676
Sand 2	293.6369	293.8601	0.93886	314.0169	313.7542	0.94357
Sand 3	294.2552	294.4784	0.94805	315.3716	315.4492	0.96608
Sand 4	293.7478	293.9710	0.94050	315.0606	315.2079	0.96286
Sand 5	293.5718	293.7950	0.93790	314.8972	314.7345	0.95655
Average	293.6341	293.8573	0.93883	314.7210	314.4582	0.95516

Note: The calibration coefficient is 0.2232 for 25°C and −0.2627 for 45°C.

well with the feature. Secondly, the emissivity difference between biogenic crust and sand decreases with temperature. The difference is 0.0272 at 25°C and decreases to 0.0178 at 45°C. Therefore, one can derive that the emissivity of sand is more sensible to temperature change than biogenic crust. This probably is because emissivity increase with temperature is not linear but exponential (Brutsaert, 1982).

Water is the most important factor shaping soil properties. The above determination of soil emissivity is based on dry samples corresponding to arid environment of the region. However, during the wet season, ground surface of the region is not absolutely dry but contains some moisture. In order to compare the impact of soil water content on its emissivity change, we also did the experiments for saturated samples. Water was filled slowly into the samples, with a fabric on the surface in order to avoid soil structure change during the process. Considering the possible temperature change during the wet season, we only conducted two temperature treatments for the wet sample experiments. The results are shown in Fig. 2b, which compares the emissivity of the soil samples in dry and saturated conditions.

As indicated in Fig. 2b, soil water eradicates the difference of possible emissivity between biogenic crust and sand. For 25°C treatment, the average emissivity at saturation is 0.9830 for biogenic crust and 0.9819 for sand. Statistical test indicates that there is no significant difference between them ($T_{\text{stat}} = 0.34 < T_{\alpha=0.1} = 1.86$). The same situation can also be seen for 35°C treatment when biogenic crust has an average emissivity of 0.9873 and sand 0.9842, which have no significant difference according to T-test ($T_{\text{stat}} = 1.09 < T_{\alpha=0.1}$). Actually, water has an emissivity of about

0.99 (Hillel, 1980; Lillesand and Kiefer, 1987; Sabins, 1996). When soil moisture increases, the thermal properties of the soil will shift from dry soil values to the water ones (Marshall and Holmes, 1979). At saturation, soil water content reaches the maximal level. When soil porosity is high such as the case in sand and soft biogenic crust, the thermal properties of soil water at saturation prevails over those of soil in dry condition. This is why the emissivity of biogenic crust and sand tends to be identical at saturation.

Even though the biogenic crust and sand totally account for above 85% of the ground surface of the region, the emissivity of other two patterns (vegetation and playa) is also required to consider for determination of average emissivity on both sides of the region.

Shrub is the dominant vegetation form of the region. The emissivity of vegetation can be found from many studies because vegetation is very important in shaping the environmental quality of the Earth's surface. Idso et al. (1969) determined the emissivity values of a number of different plant leaves and found the emissivity ranges from 0.957 to 0.995. Davies and Idso (1979, pp. 183–210) concluded that most canopy emissivity values were likely to lie between 0.96 and 0.98 and believed that a value of 0.98 was suitable in most radiation balance calculations. Humes et al. (1994) summarized the reported emissivity of vegetation as follows: grass with partial cover 0.956, shrub with partial cover 0.976 and with complete cover 0.986. Labed and Stoll (1991a, b) got the emissivity of grassland (≈ 15 cm) 0.983 and brushes (≈ 100 cm) 0.994 according to their field measurements. Price (1984) reported that the emissivity of crops in agricultural field is in general 0.96–0.98. Since our region is an arid region and many arid shrubs are in dormancy during the hot summer, we use the value of 0.978 as the average emissivity of the shrubs in the region.

As indicated above, playa of the region is similar to a silt–clay soil. Many studies reported that clay soil has an emissivity of about 0.96–0.97 (Kahle, 1980, pp. 257–273; Koorevaar et al., 1983). For the study, the playa only accounts for a small fraction ($<5\%$) of the ground and hence has little contribution in shaping the average LST change on both sides. Thus, an average emissivity of 0.965 will be used for playa in the following computation.

3. Ground temperature measurements

Documentation of ground surface temperature changes for the arid ecosystem has not been presented in the literature. In order to examine the thermal anomaly of the ecosystem to understand its occurrence, we conducted a series of ground temperature measurements in the region. Since the region can be viewed as composed of four main components: biogenic crust, sand, playa and vegetation, and the Israeli side is mainly covered with biogenic crust and various shrubs while the Egyptian side with bare sand (Pinker and Karnieli, 1995; Karnieli, 1997), the observed thermal anomaly can be thought of as a direct result of different surface compositions. It thus is necessary to carry on the measurements of ground temperature changes of the four typical surfaces for further modeling and analysis.

3.1. Methods and instruments for the measurements

The measurements were done using an IR thermometer operating in 8–14 μm. The output of the thermometer is radiant surface temperature (RST). The advantage of using IR thermometer for the measurements is that it has the ability of quickly (in 2–3 s) responding to the thermal radiance of the target when pointing to it and the output is paralleled to what is obtained in remote sensing. The output frequency of the thermometer is one record per second. A datalogger and a storage module were used to record the output of the thermometer.

The measurements were conducted at the Nizzana Research Site (Fig. 1a) on the Israeli side. Several measurements on surface temperature change had been conducted in different times and different seasons during 1997/98. A number of sampling sites representing the main surface patterns had been selected for the measurements. In order to have a comparable result of the measurements, the sampling sites were selected to be adjacent to each other within a small area and the measurements were conducted in a period of about 30–45 min so that the effect of different measuring time can be minimized. As for the measurement at each sampling site, the thermometer was pointed to the ground at the height of about 1 m with a viewing angle close to nadir. The actual measuring time for each site is about 15–20 s so that at least 10–15 data were recorded for that site. The recorded data were then downloaded into computer for analysis. Average temperature was computed for each sampling site.

Since the IR thermometer measures the radiance of ground surface to determine its radiance temperature and the thermal radiance reaching the sensor of the thermometer is not only the emittance from ground surface but also the air emittance reflected by the surface, the obtained RST must be corrected to get the true kinetic surface temperature (KST). The correction is possible only when spectral response function of the IR thermometer and the emissivity are known. In our case, we will use the emissivities determined in Section 2.2 for the correction. Since the emissivity determination is not based on the actual field measurements under natural conditions but on the indoor laboratory experiments, the correction in the following can only be termed as an approximation.

The approximation of RST measurements into KST can be based on the Stefan–Boltzmann law or Planck radiance function. Simulation results indicate that the two methods have a difference of $\sim 0.1^{\circ}$C at low temperature (15°C) and of $\sim 0.4^{\circ}$C at high temperature (55°C). Since our measurements were conducted with an IR thermometer operating in the wavelength of 8–14 μm, we prefer to base the approximation on Planck function in order to have a better accuracy. For a temperature T, we can compute Planck radiance as

$$B(T) = \frac{c_1}{\lambda^5 (e^{c_2/(\lambda T)} - 1)}, \tag{7}$$

where $B(T)$ is Planck radiance ($W\,m^{-2}$) of the ground, c_1 and c_2 are the first and the second spectral constants, and λ is effective wavelength. The IR thermometer measures the target's temperature through detecting its radiance intensity and

converting the observed radiance into temperature with a blackbody emissivity ($\varepsilon = 1$). The total thermal radiance reaching the IR thermometer I can be divided into three components: ground emittance I_g, the reflected downward atmospheric emittance I_{ar} and upward atmospheric emittance $I_a^{\uparrow}$. Mathematically, we have

$$I = I_g + I_{ar} + I_a^{\uparrow}. \tag{8}$$

The term I_{ar} depends on the ground emissivity and the downward atmospheric emittance $I_a^{\downarrow}$, generally expressed as

$$I_{ar} = (1 - \varepsilon) I_a^{\downarrow}, \tag{9}$$

where $I_a^{\downarrow}$ is the downward atmospheric emittance, which is strongly dependent on the effective atmospheric mean temperature and the atmospheric vapor content and its distribution in the profile. In remote sensing, the value can be approximated as

$$I_a^{\downarrow} = (1 - \tau_\lambda) B_\lambda(T_a^{\downarrow}), \tag{10}$$

where τ_λ is atmospheric transmittance at wavelength λ and $B_\lambda(T_a^{\downarrow})$ is the Planck radiance function. Simulation indicates that the magnitude of $B_\lambda(T_a^{\downarrow})$ ranges from 3.588 to 4.236 $\mathrm{W\,m^{-2}}$ at $T_a^{\downarrow} = 10$–$20^{\circ}\mathrm{C}$ for the wavelength 8–14 μm. Since the region is an arid region and atmospheric water vapor is low (usually $< 2\,\mathrm{g\,cm^{-2}}$), the atmospheric transmittance is high. Assumed $\tau_\lambda = 0.8$, the $I_a^{\downarrow}$ is estimated to be only about 0.72–0.84 $\mathrm{W\,m^{-2}}$. Furthermore, the ground emissivity of the region is about 0.95–0.97, which consequently results in the magnitude of the term I_{ar} quite small compared with the term I_g. Numerically, I_{ar} is estimated to be about 0.6–0.8% of I_g in our region. The small portion of I_{ar} in comparison with I_g makes the simplification of computing KST from the measured RST possible. Moreover, the distance between the ground and the IR thermometer is only about 1 m, which makes the item $I_a^{\uparrow}$ too small to be considered. Thus, we have

$$I = I_g + I_{ar} \approx 1.007 I_g. \tag{11}$$

Substituting the total radiance observed by the IR thermometer $I = B(T_r)$ and the ground emittance $I_g = \varepsilon B(T_k)$ and using Eq. (7) for Planck radiances $B(T_r)$ and $B(T_k)$, we obtain the following experimental formula for approximating T_k from the observed RST in our region:

$$T_k = \frac{c_2}{\lambda \ln(1.007\varepsilon(e^{c_2/\lambda T_r} - 1) + 1)}, \tag{12}$$

where T_r is the observed RST of the ground (K), T_k is the true KST of the ground (K), c_2 is the second spectral constant with $c_2 = 1.43876869 \times 10^{-2}\,\mathrm{m\,K}$, ε is ground emissivity, and λ is the effective mean wavelength of the IR thermometer with $\lambda \approx 12.15\,\mu\mathrm{m}$.. Therefore, knowing the emissivity, the observed RST can be easily corrected into KST. The determination of emissivity for the main surface patterns of the region has been addressed in Section 2. The corrected results of the ground temperature measurements on surface temperature of the region are presented as follows.

3.2. Surface temperature change in hot dry season

The climate of the region is typically Mediterranean, with two distinctive seasons: dry and wet. Dry season usually starts in May and ends in October though annual vibration is obvious. The rest of the year is defined as wet season though rain events during the season are very few. During dry season, there is no rain and the sky is very clear. Ground surface of the arid region is very hot at noon and June. July and August are the hottest months of the year.

Fig. 3 represents the typical KST change of the region during hot dry season. There is an obvious KST difference among the surface patterns. Biogenic crust has the highest KST and vegetation the lowest. The average KST of biogenic crust is 53.7°C (some sampling sites even reach up to 55°C). KST of playa is slightly higher than that of sand. Average KST of playa is also high (51.0°C) and that of sand is 50.6°C (Fig. 3a).

The KST difference between biogenic crust and sand is very obvious and it is high up to 3.1°C at noon (Fig. 3a). The KST of biogenic crust is also about 2.7°C higher than that of playa. *T*-test indicates that the KST differences between biogenic crust and sand and between biogenic crust and playa are both statistically significant at the level $\alpha = 0.01$ (Table 2). Another feature is the sharp KST difference between shrub canopy and its surrounding surface. According to the measurement, the difference is up to 10–15°C (Fig. 3a), which is statistically significant (Table 2). This implies that the evapo-transpiration from vegetation still controls its canopy KST change even though desert shrubs have some special functions to reduce their water lose during hot summer (Danin, 1991).

Similar features of KST change can also be seen in Fig. 3b. The KST difference among the four surface patterns is also statistically significant (Table 2). The average KST of biogenic crust is about 51.5°C, which is 2.5°C higher than that of sand and about 2.3°C playa and 13.8°C plant. Please note that the measurement was taken at the time a little bit ahead of the temperature peak at noon. According to the changing trend of the measurement, the difference at the noon peak period may reach the level of above 3°C between biogenic crust and sand. A gradual ascending of KST change can be clearly seen during the measurement period. For biogenic crust, the KST ascends from about 51.0°C at the beginning to 52.6°C at the end of the measurement. The KST of sand, playa and plant also shows some increase trends during the measurement (Fig. 3b).

Special comparison of KST change between biogenic crust and sand is presented in Fig. 3c, which represents the typical KST change of the two surface patterns in the afternoon during hot summer. The ground surface experiences a cooling process in afternoon due to the decrease of global radiation. For biogenic crust, KST decreases about 2.5°C within half an hour of the measurement. It seems that the cooling speed of sand is almost the same as biogenic crust (Fig. 3c). Again, the temperature difference between the two surfaces is very obvious and *T*-test indicates that the difference is statistically significant (Table 2). In average, it is about 2.1°C, about 1°C less than that at noon (Fig. 3a).

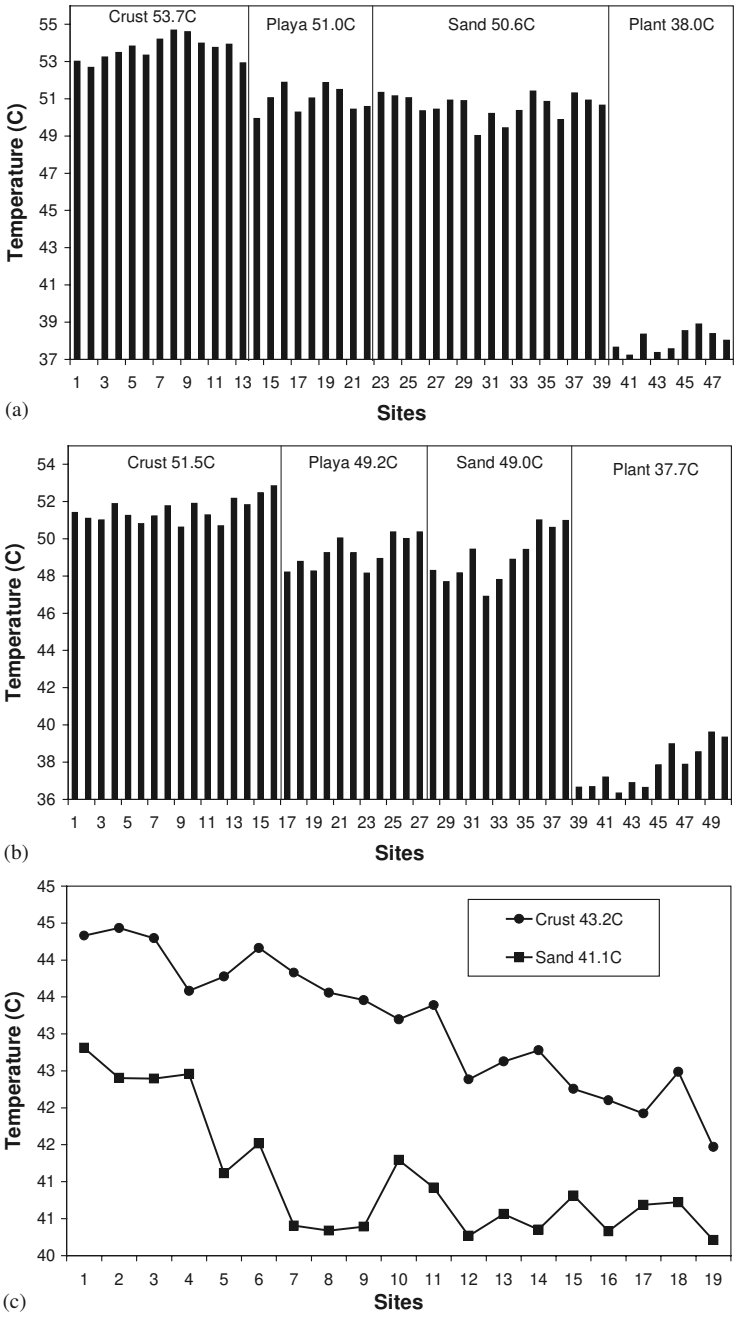

Fig. 3. KST of typical surfaces during hot dry season, (a) 13:32–14:05, June 18, 1997, (b) 11:30–12:15, August 1, 1998 and (c) 16:15–16:48, June 18, 1997.

Table 2
T-test of KST differences between surface patterns

Measurements	T_{stat} value				
	Crust–sand	Crust–playa	Crust–plant	Playa–sand	Sand–plant
13:32–14:05, 06-18-97	9.53	12.75	59.49	2.03**	47.53
16:15–16:48, 06-18-97	13.57				
11:30–12:15, 08-01-97	7.93	6.28	40.25	1.96**	21.15
09:00–09:25, 01-16-98	7.49		11.12		16.15
10:00–10:35, 01-25-98	1.06#		26.26		33.16

Note: #Statistically insignificant at level $\alpha = 0.1$; **statistically significant at level $\alpha = 0.05$; others significant at $\alpha = 0.01$.

3.3. Surface temperature change in cool wet season

Annual precipitation of the region is 95 mm (Kidron and Yair, 1997) and most of the rainfall concentrates during 1 or 2 months (Evenari et al., 1971). These characteristics make other months of wet season not really wet. The measurement shown in Fig. 4 represents KST change of the region during very wet conditions. There was a strong rain with total precipitation of 30.5 mm from January 5 to January 12, 1998. The KST shown in Fig. 4a was measured on the 5th day after the rain. The measurement time was in the morning between 9:00 and 9:25. The ground was obviously wet. Some low places still had some water puddles. After the rain, the microphytes on the crust surface became active. Several relatively dry sites were selected for the measurement of KST change.

The measurements (Fig. 4a) show that the sand has a KST of higher than that of the biogenic crust. The average KST of sand is 20.3°C, which is 1.5°C greater than that of biogenic crust (18.8°C). *T*-test indicates that the difference is statistically significant (Table 2). High soil water content after rain may be the key reason leading to this phenomenon. We all know that evaporation from the surface controls the temperature change of ground surface. This implies that the very wet surface conditions wipe the potential KST difference between the two surface patterns. Water is a critical factor that shapes the soil properties for heat transfer (Marshall and Holmes, 1979). In a short time after the rain, the soil under the surfaces is filled with a lot of water. The high content of soil water may prove to be the dominant factor in heat transfer on both surfaces. Soil porocity of bare sand is greater than that of biogenic crust. Under sunshine, the surface of bare sand experiences a process of quickly drying, leading to increase of surface temperature. Smaller soil porocity of biogenic crust makes its soil water transporting from lower layer faster, leading to greater evaporation and cooler surface temperature. As a result, bare sand has relatively higher surface temperature than biogenic crust under very wet conditions.

However, the canopy temperature of shrubs still remains lower than that of sand or biogenic crust (Fig. 4a). The average canopy temperature is 16.4°C, which is

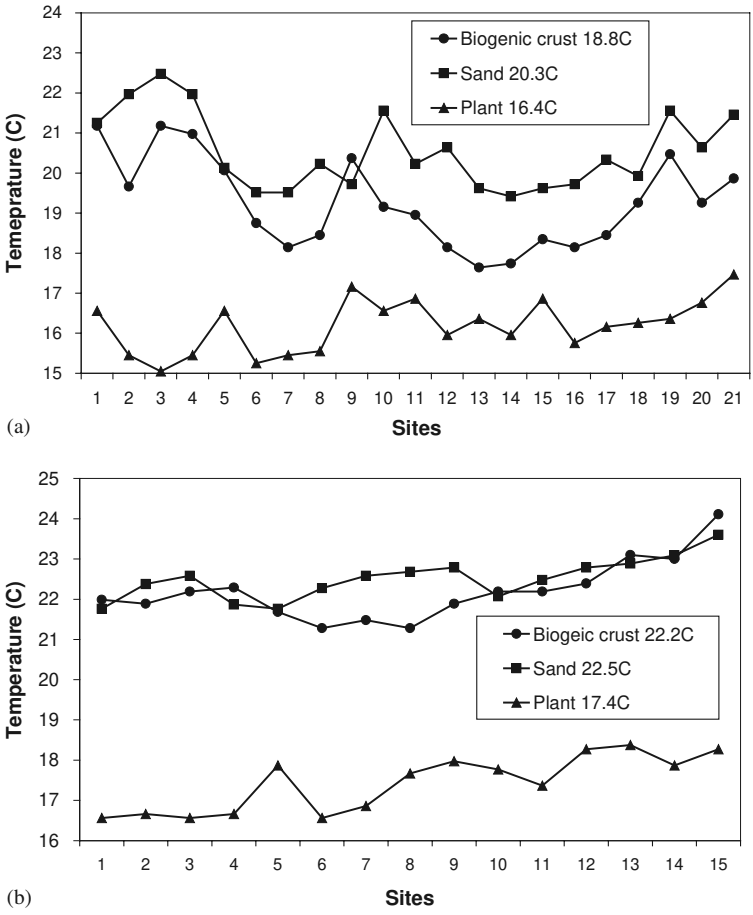

Fig. 4. True surface temperature change of typical surface patterns in very wet cool season, illustrating the measurements at (a) 9:00–9:25, January 16, 1998 and (b) 10:00–10:35, January 25, 1998. The number in the graph is the average temperature of the measurement sites.

about 3.9°C lower than the KST of sand. *T*-test indicates the difference is statistically significant (Table 2).

There was no rainfall between January 16 and 25, 1998. The results shown in Fig. 3b represent the KST changes after about 2 weeks of drying. Direct observation showed that the ground was much drier than on January 16, 1998. According to the results in Fig. 4b, the KST difference between the two main surfaces is narrowing. Higher evaporation from biogenic crust makes its soil water lose faster than bare sand. After a period of drying, soil water in biogenic crust may not be a dominant factor to cool down its surface temperature. Consequently, its surface temperature catches the level of bare sand, resulting in the disappearance of possible surface temperature difference between them. The KST during the measuring time shows a trend of gradual ascent, climbing from about 21.8°C to 24.1°C. Average KST is

22.2°C for biogenic crust and 22.5°C for bare sand. The difference is only 0.3°C, not statistically significant (Table 2). Plant canopy temperature still remains much lower than KST of biogenic crust and sand (Fig. 4b). The average canopy temperature is about 17.4°C, which is about 4.8–5°C lower than the KST of sand and biogenic crust. The differences are statistically significant according to *T*-test (Table 2).

3.4. Surface temperature change in other measurements

Except for the above two extremely dry and extremely wet situations, several additional measurements were also carried out in various seasons. Table 3 shows the results of these measurements. Similar trends can be found in all cases. There is an obvious KST difference among the four surface patterns. Biogenic crust has the highest KST, which is followed by playa and sand. Vegetation has the lowest KST among the four. On March 19, the average KST of biogenic crust was 35.1°C and that of sand was 32.8°C, with a difference of about 2.3°C. On March 26, the KST difference was about 2.8°C. The obvious KST difference can also be found in other measurements (Table 3). *T*-test indicates that the KST difference between biogenic crust and sand is statistically significant at the level of $\alpha = 0.01$. The *T*-test results in Table 4 also show that the four surfaces really have different KST though the significant level for playa–sand difference is slightly lower than others.

4. Simulation of LST change on both sides

The ground surface of the region is actually a mixture of various patterns. Moreover, the political border prevents our trip to the Egyptian side for field measurements of surface temperature change. In order to understand the LST anomaly observed in remote sensing images, average land surface temperature change across the border has to be simulated using the data from ground temperature measurements and remote sensing observation.

Table 3
Average KST of typical surface patterns in the region

Measurement time	No.	Sampling sites	Average KST (°C)			
			Crust	Sand	Playa	Plant
14:15–14:52, 05-07-97	M1	43	48.40	44.91	45.60	35.93
15:39–16:05, 05-07-97	M2	37	43.27	40.13	41.08	32.66
14:19–14:55, 10-06-97	M3	45	42.34	39.67	40.21	32.42
11:20–12:00, 03-19-98	M4	47	35.13	32.90	33.44	24.49
11:16–12:04, 03-26-98	M5	45	34.04	31.18	31.57	25.12
10:30–11:11, 04-10-98	M6	56	35.81	34.09		28.47

Table 4
T-test of KST difference between surface patterns

Measurement no.	T_{stat} value				
	Crust–sand	Crust–playa	Crust–plant	Playa–sand	Sand–plant
M1	10.33	9.04	56.66	1.93**	26.81
M2	7.86	3.53	24.12	1.99**	13.90
M3	9.27	8.14	41.46	1.56***	23.57
M4	9.44	6.63	42.36	2.13**	37.92
M5	14.89	9.56	28.89	1.34***	26.68
M6	4.34	8.86	25.49		20.08

Note: ***Significant at $\alpha = 0.1$, others significant at $\alpha = 0.05$. **Statistically significant at level $\alpha = 0.01$.

4.1. Method

Since the pixel of satellite image is usually greater than any single surface patterns in the region, the LST anomaly observed by remote sensing is in fact a phenomenon based on the mixed surface temperature within a pixel, which can be divided into several components according to the surface composition. Therefore, the principle for estimating average LST change across the border is the structural composition of the ground surface on both sides of the region. The total thermal radiance (I_s) emitted from the ground for remote sensing of LST can be written as

$$I_g = A_c I_c + A_s I_s + A_v I_v + A_p I_p + I_i, \tag{13}$$

where A_c, A_s, A_v and A_p are surface fractions of biogenic crust, sand, playa and vegetation respectively, I_c, I_s, I_v and I_p are the thermal radiances emitted from the four surface patterns, and I_i represents the interaction among the four patterns. Since the desert shrubs are sparse and generally with a height of less than 1 meter, the interaction term can be reasonably ignored in our case. Thus, the above equation can be rewritten after applying Stefan–Boltzmann law to each radiance term as follows:

$$\varepsilon\sigma T_s^4 = A_c\varepsilon_c\sigma T_{kc}^4 + A_s\varepsilon_s\sigma T_{ks}^4 + A_v\varepsilon_v\sigma T_{kv}^4 + A_p\varepsilon_p\sigma T_{kp}^4, \tag{14}$$

where σ is Stefan–Boltzmann constant; T_s is the average LST; T_{kc}, T_{ks}, T_{kv}, and T_{kp} are KSTs of biogenic crust, sand, vegetation and playa, respectively; A_c, A_s, A_v, and A_p are the surface fractions of the four components; ε is the average ground emissivity. Elimination of σ from Eq. (9) leads to the following formula for computing the average LST on both sides of the region:

$$T_s = (F_c T_{kc}^4 + F_s T_{ks}^4 + F_v T_{kv}^4 + F_p T_{kp}^4)^{1/4}, \tag{15}$$

where the coefficients F_c, F_s, F_v, and F_p are the emissivity fractions, given as $F_c = A_c\varepsilon_c/\varepsilon$, $F_s = A_s\varepsilon_s/\varepsilon$, $F_v = A_v\varepsilon_v/\varepsilon$ and $F_p = A_p\varepsilon_p/\varepsilon$. According to surface composition, the average emissivity is estimated as 0.968 for the Israeli side and 0.954 for the Egyptian side. Consequently, the fractions can be computed for estimation of average LST on both sides. Using the quantitative surface composition structure on

both sides of the region (Qin et al., 2003), the emissivity fractions are estimated as $F_c = 0.8217$, $F_s = 0.0834$, $F_v = 0.0701$ and $F_p = 0.0349$, respectively, for the Israeli side and $F_c = 0.1393$, $F_s = 0.8066$, $F_v = 0.0183$ and $F_p = 0.0354$ for the Egyptian side. Note that the fractions are estimated for the conditions of summer hot season when the vegetation canopy in the arid region reduces to minimum and the LST anomaly are observed to be very obvious across the border. With these estimates, we are able to simulate the average LST change on both sides of the region for comparison of their difference.

4.2. Simulation results and analysis

We use the above method to estimate the average LST change on both sides and their difference using the measured KST of the four surface patterns shown in Table 3. The estimated results are presented in Fig. 5. Based on the measurement given in Fig. 3a, the estimated average LST is up to 53.1°C on the Israeli side and 50.8°C on the Egyptian side, with a difference of 2.3°C. The average LST on both sides is also up to 2.0°C according to measurement shown in Fig. 3b, which was taken at the time just before noon. Because the measurement shown in Fig. 3c was taken in late afternoon, slightly lower average LST difference on both sides (1.7°C) is reasonable. Similar LST difference on both sides can be seen in early and late dry seasons. For the measurements M1–M3 in Table 3, average LST difference is found to be up to 2.3–2.8°C (Fig. 5). However, the reverse LST difference on both sides exists in wet season when temperature is low. Due to very wet surface after heavy rain, the average LST of Figs. 4a and b is estimated to be about 20°C and 23°C on both sides (Fig. 5). Consequently, the LST difference on both sides is −0.3°C and 0.3°C, respectively. The estimation results suggest that the LST anomaly is strongly related to temperature level. The anomaly becomes more obvious when the temperature

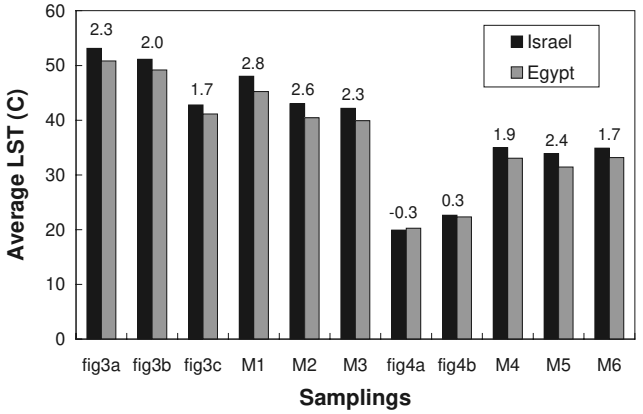

Fig. 5. Average LST change on both sides of the region, estimated from the measurements taken at Nizzana Research Site. The number in the graph is average LST difference on both sides. The samplings M1–M6 refer to the measurements in Table 3.

level is high such as shown in the measurements of M1–M3. The average LST difference between the Israeli and the Egyptian sides reduces to minimum when the temperature level is at around 20°C as shown by the measurements in Fig. 4b.

In order to verify this conclusion, we extend our estimation of the average LST and its difference across the border into a systematic simulation, using a reasonable combination of the KST of the four surface patterns according to the ground temperature measurements. First of all, we try to determine the relationship between LST difference on both sides and the crust–sand KST difference. Then we try to answer the question: under what temperature level does the LST anomaly appear across the border in the region?

Fig. 6a shows the change of the estimated LST difference on both sides of the region with temperature for various crust–sand KST differences. Two features can be clearly seen from Fig. 6a. The Israeli side has an average LST higher than the Egyptian side only when biogenic crust has a LST of $>1°C$ higher than bare sand. In summer, surface temperature of the region is usually in the range of 40–57°C at about noon during daytime. The ground temperature measurements indicate that biogenic crust usually has a KST of above 3°C higher than that of sand. For this condition, the average LST difference on both sides will be $>2.5°C$. In other words the Israeli side has an average LST of at least 2.5°C higher than the Egyptian one during hot dry season. Specifically, when biogenic crust is about 4°C hotter than sand, the average LST difference on both sides will be about 3°C. This is accordance with what was obtained on remote sensing analysis of LST (Qin et al., 2002a).

In winter and during night-time, surface temperature of the region is usually low. The difference of surface temperature between biogenic crust and sand is not as obvious as that under hot dry condition. If the crust–sand KST difference is below $-1°C$, the average LST on the Israeli side will be lower than the Egyptian side. As shown in Fig. 6a, the average LST difference on both sides is about $-0.6°C$ when biogenic crust is about $-1°C$ cooler than sand. This implies that in low temperature such as several days after the heavy rain and winter night-time the Egyptian side probably has slightly higher LST than the Israeli side. However, if biogenic crust and sand have no difference in their surface temperature, the Israeli and the Egyptian sides will also have no significant difference in their average LST. This result also verifies the result of remote sensing analysis to the LST change on both sides from AVHRR and Landsat TM data (Qin et al., 2002a).

Fig. 6b shows the simulation results of average LST change on both sides of the region in corresponding to the possible temperature change (represented by biogenic crust KST) in the region. Linear characteristic of the change is clear. Generally, the Israeli side will have a higher average LST than the Egyptian side in high temperature ($>30°C$). In very low temperature ($<15°C$), the Egyptian side will have steadily higher average LST than the Israeli side though the difference is still weak ($<-1.0°C$). Another important feature shown in Fig. 6b is that the average LST difference on both sides is not obvious, vibrating between $-0.5°C$ and $0.5°C$ (also see Fig. 6c), in temperature range 15–25°C. Usually LST of the region is within this range at about midnight. This is why we are not able to observe an obvious LST anomaly of the region on the night-time remote sensing images of NOAA-AVHRR

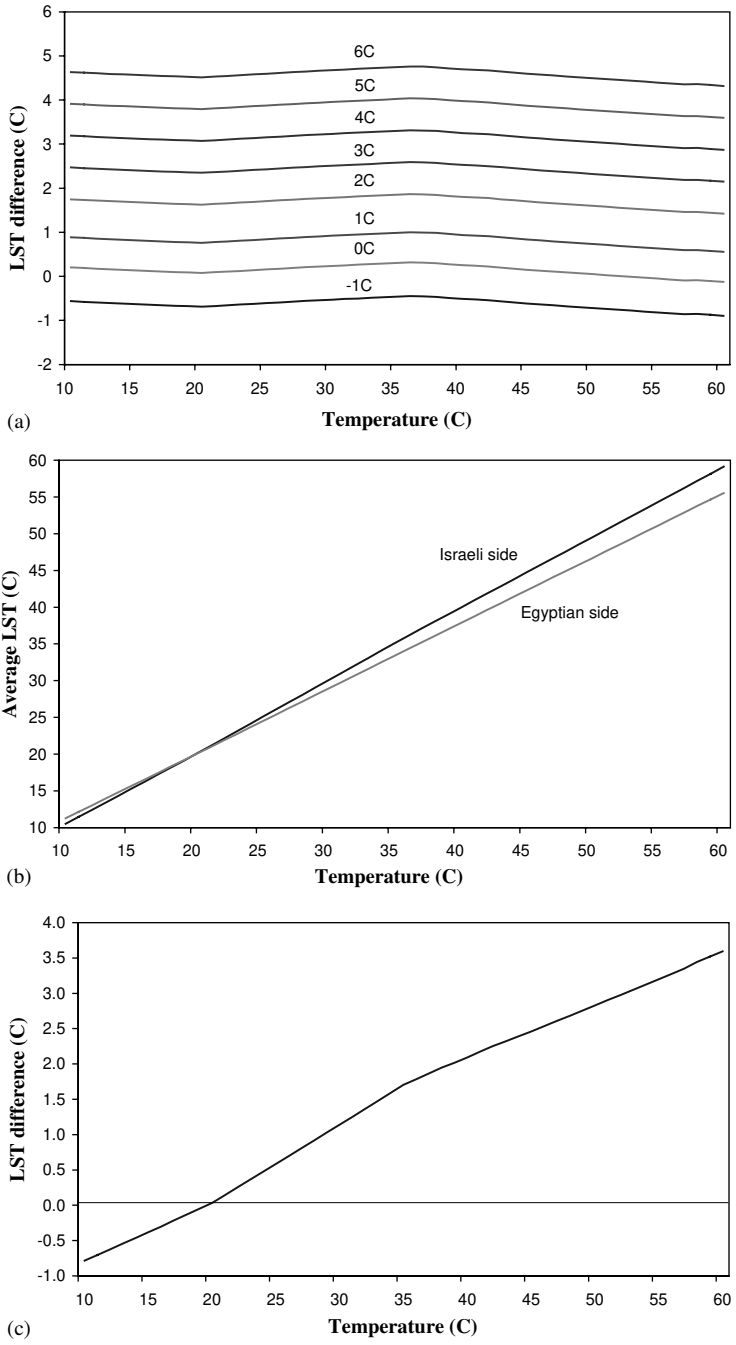

Fig. 6. Simulation results of average LST change and its difference on both sides of the region, (a) the effect of KST difference (the number in the graph) between biogenic crust and sand, (b) the possible average LST change and (c) its difference on both sides of the region.

(Qin et al., 2002a). The change of possible average LST difference between the two sides is clearly shown in Fig. 6c, which is computed from the simulation results of Fig. 6b. Specifically, the LST difference may reach 2.5–3.5°C when temperature of biogenic crust is in the range of 45–55°C, which is the general case in hot dry season. Therefore, we are sure that the ground truth measurement of surface temperature verifies the LST anomaly across the border observed by remote sensing imagery. And the simulation reveals the conditions of ground surface temperature for the occurrence of the thermal anomaly across the political border.

5. Conclusion

Ground emissivity plays an important role in thermal emittance of the ground surface. According to the experiments and analysis, it can be concluded that the average emissivity of the biogenic crust and the sand is separately 0.97 and 0.95 in dry condition. Both the biogenic crust and the sand samples behave a weak increase of emissivity with temperature. The sand seems to have slightly greater increase pace than biogenic crust. Comparison has also been done to the emissivity of the samples in dryness and saturation. The result indicates that the difference of emissivity between the biogenic crust and the sand samples in dry condition seems to disappear at saturation when soil water governs the thermal properties of the soil. At saturation, both the biogenic crust and the sand samples have high and close high emissivity of up to 0.982–0.983 for the treatment at 25°C and 0.984–0.987 at 35°C.

The ground temperature measurements during 1997–1998 indicate that an obvious difference of surface temperature does exist between biogenic crust and sand in most days of the year. In dry summer at about noon, biogenic crust has higher KST than sand. In morning and afternoon, the difference is smaller but also overt. In early and late dry seasons, the difference is still above 2.5°C at about noon. The difference reverses only in a few days after heavy rain when the biogenic crust is very wet or at higher water content while the bare sand surface is relatively drier. Under this extreme condition, the bare sand has an average KST of about 1°C higher than the biogenic crust (Fig. 4a). The lower KST of biogenic crust is due to the fact that soil water content strongly shapes its thermal properties. However, the reverse KST difference between the two main surfaces becomes very weak after about 2 weeks of strong rain (Fig. 4b).

Shrub canopy has the lowest canopy temperature in all seasons. The difference of shrub canopy temperature from biogenic crust KST may reach up to 15°C at noon, as indicated in Fig. 3a. During the wet season when the KST difference between biogenic crust and sand surface reverses due to the wetter surface of biogenic crust, shrub canopy temperature still remains about 4°C lower than KST of sand, as indicated in Fig. 4a. The obvious lower canopy temperature than surrounding environment demonstrates that evapo-transpiration still functions to cool down desert plants though the plants may remain in a status of semi-dormancy to minimize their evapo-transpiration.

Using the structural composition of ground surface and its relationship with the thermal radiance, we develop a simple method to estimate the average LST change on both sides of the region. The estimation with the ground truth measurement data indicates that the observation of the LST anomaly on remote sensing imagery does exist in the sand dune region. As verified by the measurement shown in Fig. 3 and M1–M3, the Israeli side is above 2°C hotter than the Egyptian side. The average LST difference disappears in measurements shown in Fig. 4, which represents the very wet conditions after the heavy rain.

Therefore, the observed LST anomaly of the arid ecosystem is mainly attributed to the difference of surface composition on both sides of the border. This surface composition difference, together with their emissivity difference, plays an important role in shaping LST change across the region. The Israeli side has about 72% surface covered with biogenic crust while the Egyptian side has above 4/5 surface belonging to bare sand. The much greater fraction of biogenic crust on the Israeli side determines its much higher average LST change. And the much greater fraction of bare sand on the Egyptian side explains its relatively lower average LST change. Even though there is a sharp difference of vegetation cover rate on both sides, its very low fraction in estimating average LST change does not contribute a lot to even the sharp LST contrast produced by great difference of biogenic crust and bare sand on both sides. As a result, the Israeli side is notably hotter than the Egyptian side. Our study of this thermal anomaly reveals an important principle regarding the thermal relationship between vegetation cover and surface temperature of arid ecosystem: more vegetation under arid environment may not guarantee a relatively cooler surface due to the low percentage of desert plants' evapo-transpiration in the surface energy balance of the ecosystem.

Acknowledgements

The authors sincerely thank the following persons for their various help in conducting our research and preparing the paper: Dr. Heike Schmid, our colleague at the Remote Sensing Laboratory, for helping to access the region for ground temperature measurements; Mr. Giorgio Dall' Olmo and Ms. Svetlana Gilerman, our colleagues, for assistance of some image processing; Mr. Simon Berkowics, administrator of The Arid Econsystems Research Center, Inst. of Earth Sciences, The Hebrew University of Jerusalem, for offering the permission to conduct ground temperature measurements at the Nizzana Research Site and providing useful information about researches on the region; Dr. Axel Allaier and Dr. Thomas Litmann from Germany, Mr. Gil Revivo, Dr. Robi Stark and Mr. Guy from Ben Gurion University of the Negev for personal communication about the region; Ms. Emily Oklay from University of California at Davis, USA for checking the English. And finally, the publication of the paper is supported by China 973 project 2001CB309404 and CAAS Outstanding Scientist Foundation.

References

Balling Jr., R.C., 1989. The impact of summer rainfall on the temperature gradient along the United States-Mexico border. Journal of Applied Climatology 28, 304–308.

Balling Jr., R.C., Klopatek, J.M., Hildebrandt, M.L., Moritz, C.K., Watts, C.J., 1998. Impacts of land degradation on historical temperature records from the Sonoran desert. Climatic Change 40, 669–681.

Brutsaert, W., 1982. Evaporation into the Atmosphere: Theory, History and Application. D. Reidel Publishing Company, Dordrecht, The Netherlands, 299pp.

Caselles, V., Coll, C., Valor, E., 1997. Land surface emissivity and temperature determination in the whole HAPES-Sahel area from AVHRR data. International Journal of Remote Sensing 18, 1009–1027.

Danin, A., 1991. Plant adaptation in desert dunes. Journal of Arid Environment 21, 193–212.

Davies, J.A., Idso, S.B., 1979. Estimating the surface radiation balance and its components. In: Barfield, B.J., Gerber, J.F. (Eds.), Modification of the Aerial Environment of Plants. American Society of Agricultural Engineers, St. Joseph, Michigan, USA, 538pp.

Evenari, M., Shana, L.Tadmor, N., 1971. The Negev—The Challenge of a Desert. Harvard University Press, Cambridge, MA, USA, 265pp.

Gerson, R., Amit, R., Grossman, S., 1985. Dust Availability in Desert Terrain: A Study in the Deserts of Israel and the Sinai. The Hebrew University of Jerusalem, Jerusalem, Israel, 63pp.

Hausenbuiller, R.I., 1978. Soil Science: Principles and Practices. Wm C. Brown Company, Dubuque, IA, USA, 251pp.

Hillel, D., 1980. Fundamentals of Soil Physics. Academic Press, New York, USA, 209pp.

Humes, K.S., Kustas, W.P., Moran, M.S., Nichols, W.D., Weltz, M.A., 1994. Variability of emissivity and surface temperature over a sparsely vegetated surface. Water Resources Research 30 (5), 1299–1310.

Idso, S.B., Jackson, R.D., Ehrler, W.L., Mitchell, S.T., 1969. A method for determination of infrared emittances of leaves. Ecology 50, 899–902.

Kahle, A.B., 1980. Surface thermal properties. In: Siegal, B.S., Gillespie, A.R. (Ed.), Remote Sensing in Geology. Wiley, New York, USA, 385pp.

Karnieli, A., 1997. Development and implementation of spectral crust index over dune sands. International Journal of Remote Sensing 18, 1207–1220.

Karnieli, A., Sarafis, V., 1996. Reflectance spectrophotometry of cyanobacteria within soil crusts—a diagnostic tool. International Journal of Remote Sensing 17, 1609–1615.

Karnieli, A., Tsoar, H., 1995. Spectral reflectance of biogenic crust developed on desert dune sand along the Israel–Egypt border. International Journal of Remote Sensing 16, 369–374.

Karnieli, A., Shachack, M., Tsoar, H., Zaady, E., Kaufman, Y., Porter, W., 1996. The effect of microphytes on the spectral reflectance of vegetation in semi-arid regions. Remote Sensing of Environment 57, 88–96.

Kidron, G.J., Yair, A., 1997. Rainfall–runoff relationship over encrusted dune surfaces, Nizzana, Western Negev, Israel. Earth Surface Processes and Landforms 22, 1169–1184.

Koorevaar, P., Menelik, G., Dirksen, C., 1983. Elements of Soil Physics. Elsevier Science Publishers, Amsterdam, The Netherlands, 169pp.

Labed, J., Stoll, M.P., 1991a. Angular variation of land surface spectral emissivity in the thermal infrared: laboratory investigations on bare soils. International Journal of Remote Sensing 12 (11), 2299–2310.

Labed, J., Stoll, M.P., 1991b. Spatial variability of land surface emissivity in the thermal infrared band: spectral signature and effective surface temperature. Remote Sensing of Environment 38 (1), 1–17.

Lillesand, T.M., Kiefer, R.W., 1987. Remote Sensing and Image Interpretation. Wiley, New York, 325pp.

Marshall, T.J., Holmes, J.W., 1979. Soil Physics, Cambridge University Press, Cambridge, UK, 268pp.

Otterman, J., 1974. Baring high-albedo soils by overgrazing: a hypothesized desertification mechanism. Science 186, 531–533.

Otterman, J., 1977. Anthropogenic impact on the surface at the Earth. Climatic Change 1, 137–155.

Otterman, J., 1981. Satellite and field studies of man's impact on the surface in arid regions. Tellus 33, 68–77.

Otterman, J., Robinove, C.J., 1982. Landsat monitoring of desert vegetation growth in 1972–1979 using a plant shadowing model. Advance of Space Researches 2, 45–50.

Otterman, J., Tucker, C.J., 1985. Satellite measurements of surface albedo in semi desert. Journal of Climate and Applied Meteorology 24, 228–235.

Pinker, R.T., Karnieli, A., 1995. Characteristic spectral reflectance of a semi-arid environment. International Journal of Remote Sensing 16, 1341–1363.

Price, J.C., 1984. Land surface temperature measurements from the split window channels of the NOAA 7 advanced very high resolution radiometer. Journal of Geophysical Research 89, 7231–7237.

Qin, Z., Berliner, P., Karnieli, A., 2001. Thermal variation in the Israel–Sinai (Egypt) peninsula region. International Journal of Remote Sensing 22 (6), 915–919.

Qin, Z., Karnieli, A., Berliner, P., 2002a. Remote sensing analysis of the land surface temperature anomaly in the sand dune region across the Israel–Egypt border. International Journal of Remote Sensing 23 (19), 3991–4018.

Qin, Z., Berliner, P., Karnieli, A., 2002b. Micrometeorological modeling to understand the thermal anomaly in the sand dunes across the Israel–Egypt border. Journal of Arid environment 51 (2), 281–318.

Qin, Z., Li, W., Karnieli, A., Berliner, P., 2003. Quantitative estimation of land cover structure in the desert sand dunes across Israel–Egypt border using remote sensing data. IEEE 2003 International Geosciences and Remote Sensing Symposium, III: 1879–1881, July 21–25, 2003, Toulouse, France.

Sabins, F.F., 1996. Remote Sensing: Principles and Interpretation. W.H. Freeman, New York, USA, 386pp.

Sobrino, J.A., Caselles, V., 1991. A methodology for obtaining the crop temperature from NOAA-9 AVHRR data. International Journal of Remote Sensing 12 (12), 2461–2475.

Sobrino, J.A., Raissouni, N., Li, Z.L., 2001. A comparative study of land surface emissivity retrieval from NOAA data. Remote Sensing of Environment 75 (2), 256–266.

Tielböger, K., 1997. The vegetation of linear desert dunes in the northwestern Negev, Israel. Flora 192, 261–278.

Tsoar, H., 1990. Grain-size characteristics of wind ripples on a desert sand dune. Geographic Research Forum 10, 37–50.

Tsoar, H., Karnieli, A., 1996. What determines the spectral reflectance of the Negev–Sinai sand dunes. International Journal of Remote Sensing 17, 3513–3525.

Tsoar, H., Møller, J.T., 1986. The role of vegetation in the formation of linear sand dunes. In: Nickling, W.P. (Ed.), Aeolian Geomorphology. Allen & Unwin Inc., Boston, USA, 327pp.

Warren, A., Harrison, C.M., 1984. People and the ecosystem: biogeography as a study of ecology and culture. Geoforum 15, 365–381.